Power Flow Analysis of a Grid-Connected High-Voltage Microgrid with Various Distributed Resources

Wei-Tzer Huang
Department of Electrical Engineering, Chienkuo Technology University
No.1, Chieh Shou N. Rd., 500 Changhua City, Taiwan
vichuang@ctu.edu.tw

Wen-Chih Yang
Department of Electrical Engineering, Technology and Science Institute of Northern Taiwan
No. 2, Xueyuan Rd., Peitou, 112 Taipei, Taiwan
wcyang@tsint.edu.tw

Abstract—**This paper aims to analyze the power flow of a grid-connected 11.4 kV high-voltage microgrid (MG) with various distributed resources (DRs). First, related papers and technological reports were extensively surveyed. Accordingly, five different types of DRs and their controllable loads were considered for integration into two 11.4 kV primary feeders. These DRs include two 1.5 MW diesel engine generators, two 1.79 MW gas turbine generators, two 1.0 MW fuel cell generation systems, a 1.5 MW wind turbine generator, and a 0.5 MW photovoltaic generation system. Second, using the Newton-Raphson method, we developed a sequential power flow program in Matlab environment and verified its accuracy. Finally, the program was used to simulate and analyze the power flow of an MG for one 24-hour period under the grid-connected operating mode. The outcomes of this paper should prove helpful for distributed engineers to further understand the behaviors and characteristics of high-voltage MGs.**

Keywords- Microgrid, Distributed Resources, Power Flow, Steady-State Analysis, Grid-Tie Operation.

I. INTRODUCTION

The goal of the Kyoto Protocol [1] is to lower overall emissions from greenhouse gases, i.e., carbon dioxide, methane, nitrous oxide, sulfur hexafluoride, HFCs, and PFCs. Through these measures, member nations aim to effectively curb the occurrence of global warming. Even with such measures in place, however, global warming remains a serious problem, and disasters borne of abnormal climates continue to occur. Global warming and its implications on important world issues have received considerable attention. The sustainable development of human civilization has become a critical issue, prompting 192 nations to convene for the United Nations Climate Change Conference in Copenhagen on 7 December 2009. Climate change mitigation was extensively discussed with the hope of establishing climatic change protocols.

Greenhouse gas emissions stem from human activities in different sectors, such as the generation, transportation, industrial, and agricultural industries, among others. As for electrical power systems, reducing generation-related greenhouse gas emissions is a most important task. Thus, decreasing the proportion of centralized large thermal units and increasing the use of renewable energy resources will be helpful in reducing harmful emissions. Additionally, these measures can effectively improve the overall operations and efficiency of existing power systems, and moderate the expansion of large-scale power plants and transmission systems. On the basis of these objectives, we infer that the development of relevant technology for distributed resources (DRs) is an unavoidable trend. DRs are usually connected to distribution networks directly supplying power to the network to satisfy customer demands. Consequently, the incorporation of DRs reduces total power system loss because no transmission losses are incurred, and DRs usually offer the advantages of low environmental effects and high efficiency. Generally, distribution networks integrated with various DRs and loads to form a small power system are called microgrids (MGs); these can be operated in grid-connected and islanding modes [2–6].

Given that MGs have become a new development trend in power systems, realizing solid system structures, as well as operating and control technologies, among others, is a necessary requirement. To this end, we study the steady-state characteristics of a high-voltage MG with five different types of DRs, namely, a wind turbine generator, photovoltaic generation system, solid oxide fuel cell, diesel engine generator, and gas turbine generator. We anticipate that the nature of the 11.4 kV high-voltage MG will be thoroughly understood after our detailed analysis of the power flow under the grid-tied operation mode.

II. DESCRIPTION OF THE HIGH-VOLTAGE MICROGRID

Fig. 1 shows a high-voltage MG, modified from a 11.4 kV primary distribution system of Taipower. This system consists of a main transformer rated at 25 MVA, 69 kV/11.4 kV, and 60 Hz, and five primary feeders. The F#1 and F#2 feeders form an MG through a point of common coupling (PCC) of the static switch that enables connection and disconnection from the upstream utility grid; the other feeders, F#3–F#5, are the normal feeders without DRs.

The F#1 and F#2 MG can also be divided into two sub-MGs, which are F#1 and F#2 high-voltage MGs. The F#1 MG is composed of two gas turbine generators (GT#1, GT#2), two

978-1-4244-9438-5/11/$26.00 ©2011 IEEE

fuel cell generation systems (FC#1, FC#2), a photovoltaic cell generation system (PV), and three types of equivalent lumped loads, which are residential, office, and commercial loads. The F#2 MG comprises two diesel engine generators (DE#1, DE#2), a wind turbine generator (WT), as well as two types of equivalent loads: residential and industrial loads.

In this paper, the MG is assumed to operate in grid-connected mode; therefore, the load demands are supplied by the DRs, purchased from the utility grid. The principle of the MG optimal dispatch is the minimization of fuel cost subject to power balance. The detailed procedure is not described here. The results of optimal real power output of each DR and grid (through the PCC) are shown in Fig. 2. Additionally, the equivalent lumped load curves for the real and reactive powers of each load types are shown in Figs. 3and 4, respectively.

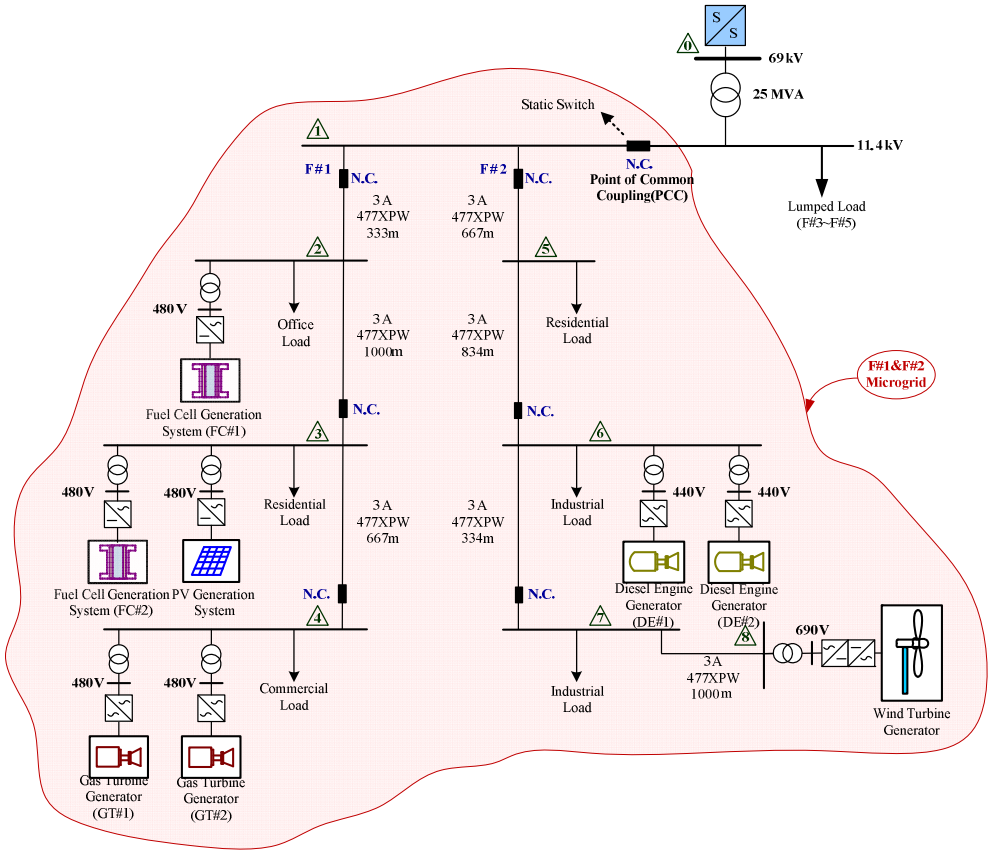

Fig. 1 System structure of the high-voltage microgrid

III. Description of the Solution Method

The Newton-Raphson method is one of the most commonly used techniques for solving nonlinear algebraic equations, and presents better convergence than does the Gauss-Seidel method. Thus, it is popularly applied in power flow analysis. The iteration numbers of the Newton-Raphson approach is independent of the scale of system and can solve the problem through a few iterations. However, its Jacobian matrix requires recalculation and updating in each iterative step [7–8]. In this paper, the loads and DRs are assumed to be equivalent injected powers in power flow analysis. Equations (1) and (2) are the power mismatches for bus i, in which $P_i^{(k),spec}$ and $Q_i^{(k),spec}$ represent the equivalent real and reactive power injections of the bus, and $P_i^{(k),cal}$ and $Q_i^{(k),cal}$ denote the calculated values of the injected real and reactive powers of the bus, respectively. These can be calculated using Eqs. (3) and (4).

$$\Delta P_i^{(k)} = P_i^{(k),spec} - P_i^{(k),cal} \tag{1}$$

$$\Delta Q_i^{(k)} = Q_i^{(k),spec} - Q_i^{(k),cal} \tag{2}$$

$$P_i^{(k),cal} = \sum_{j=1}^{n} \left|V_i^{(k)}\right|\left|V_j^{(k)}\right|\left|Y_{ij}\right|\cos\left(\theta_{ij} + \delta_j^{(k)} - \delta_i^{(k)}\right) \tag{3}$$

$$Q_i^{(k),cal} = -\sum_{j=1}^{n} \left|V_i^{(k)}\right|\left|V_j^{(k)}\right|\left|Y_{ij}\right|\sin\left(\theta_{ij} + \delta_j^{(k)} - \delta_i^{(k)}\right) \tag{4}$$

Collecting all mismatch equations into vector-matrix form yields

$$\begin{bmatrix} \Delta P_i^{(k)} \\ \Delta Q_i^{(k)} \end{bmatrix} = \begin{bmatrix} \dfrac{\partial P_i}{\partial \delta_i^{(k)}} & \dfrac{\partial P_i}{\partial \left|V_i^{(k)}\right|} \\ \dfrac{\partial Q_i}{\partial \delta_i^{(k)}} & \dfrac{\partial Q_i}{\partial \left|V_i^{(k)}\right|} \end{bmatrix} \begin{bmatrix} \Delta \delta_i^{(k)} \\ \Delta \left|V_i^{(k)}\right| \end{bmatrix} \tag{5}$$

Equation (5), which is the formula for the correction of phase angle and magnitude of bus voltages $\Delta\delta_i^{(k)}$ and $\Delta\left|V_i^{(k)}\right|$, is solved using Eq. (6), and the solved corrections are added to update all buses voltages using Eqs. (7) and (8). The power flow equations are solved until the power mismatches at all

buses fall within the specified tolerance levels, as shown in Fig. 5.

$$\begin{bmatrix} \Delta\delta_i^{(k)} \\ \Delta|V_i^{(k)}| \end{bmatrix} = \begin{bmatrix} J_1 & J_2 \\ J_3 & J_4 \end{bmatrix}^{-1} \begin{bmatrix} \Delta P_i^{(k)} \\ \Delta Q_i^{(k)} \end{bmatrix} \quad (6)$$

$$\delta_i^{(k+1)} = \delta_i^{(k)} + \Delta\delta_i^{(k)} \quad (7)$$

$$|V_i^{(k+1)}| = |V_i^{(k)}| + \Delta|V_i^{(k)}| \quad (8)$$

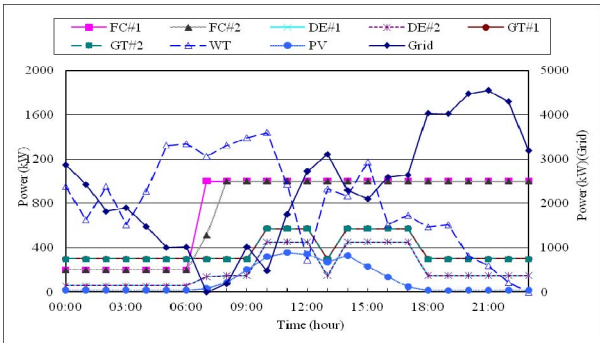

Fig. 2 Optimal real power output curves for the DRs and grid

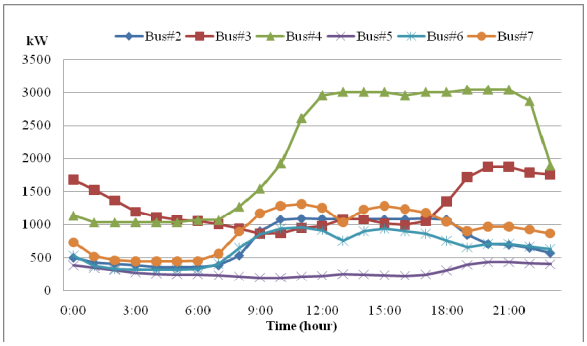

Fig. 3 Equivalent lumped load curves of real power at load buses

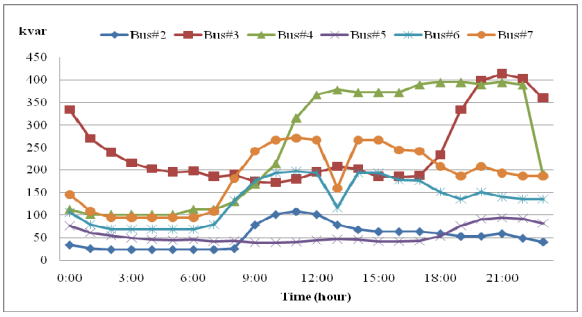

Fig. 4 Equivalent lumped load curves of reactive power at load buses

IV. Simulation Results and Discussion

In this paper, the Newton-Raphson method was applied to solve the power flow of the high-voltage MGs, F#1 and F#2 MGs, which contain renewable and non-renewable DRs under grid-connected operating mode, with the assumption that the system is three-phase balanced. A 24-hour operating analysis was explored in detail in this section, after rigorous engineering analyses and discussions on the voltage profiles, line flow profiles, and system losses. The simulation results are illustrated as follows.

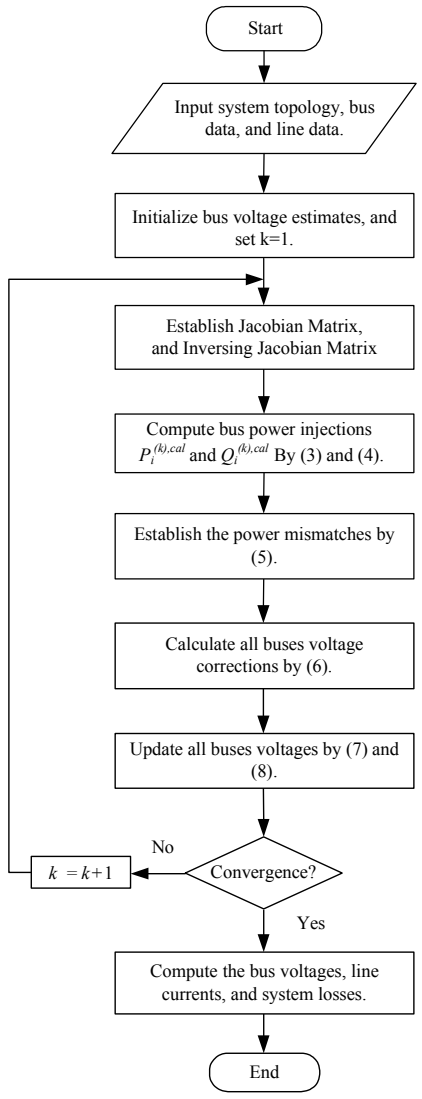

Fig. 5 Flow chart of the proposed newton-raphson method

A. Voltage Profiles

The results of the simulation on voltage profiles along feeders F#1 and F#2 are shown in Fig. 5. After the DRs were connected to the network, the power was fed not only from the upstream utility grid but also from the local DRs (Fig. 2). Therefore, the power fed from the upstream grid through the main transformer is reduced with the incorporation of the DRs. The voltage drops improve, and the average daily voltages at each bus increase. Consequently, the voltage at the end of the relatively heavier loading feeder, F#1, is greater than 0.97 p.u.; the voltage at Bus#4 is 0.986 p.u. during the peak loading period. The DRs integrated into the distribution network are clearly helpful to the system voltage profiles under suitable control constraints.

B. Line Flow Profiles

Figs. 6 and Fig. 7 depict the simulation results of real and reactive power flows in each feeder segment during one 24-hour period. The peak loading period of the MG occurs around

18:00 to 23:00; by contrast, the off-peak loading period occurs around 00:00 to 08:00. The simulation results of the voltage profiles and line flows clearly reflect these phenomena. The variations in the complex power flow are significant in each feeder segment at different times in one day. The directions of power flows in some feeder segments are reversed, especially in feeder F#2. The reversed complex power flowing in the primary feeder between buses 7 and 8 is the largest among all the feeder segments because Bus#8 is a generator bus connected to a wind turbine generator. The power supply from this bus is a function of wind velocity. Similarly, the photovoltaic cell generation system is connected to Bus#3; the power output of this bus is directly proportional to solar irradiation and cell temperature. The simulation results illustrate that the power supply by PV is approximately between 07:00 to 15:00. The power supply from the above-mentioned buses is highly dependent on weather conditions. Additionally, Figs. 6 and 7 show that the peak loads of the MG are 4604.4 kW and 1482.9 kvar, occurring at 21:00. Conversely, the off-peak loads of the MG are 48.6 kW and 548.4 kvar, occurring at 07:00. To sum up, the DRs can share load demands and lessen the power supply requirement from the upstream utility grid.

C. *System Losses*

Fig. 8 shows the total losses of the system during a 24-hour period. On the basis of the simulation results, we conclude that the power loss is directly proportional to the loading. Accordingly, the more load used, the higher the increase in losses. Furthermore, the system losses decrease because of to the incorporation of DRs in this specific system.

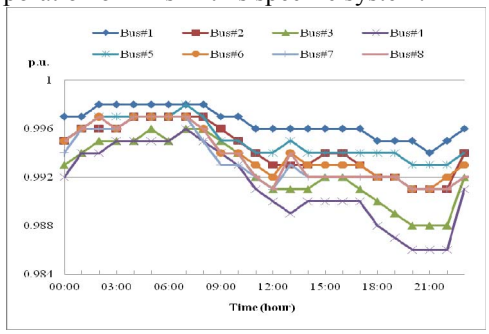

Fig. 5 Simulation results of the bus voltage

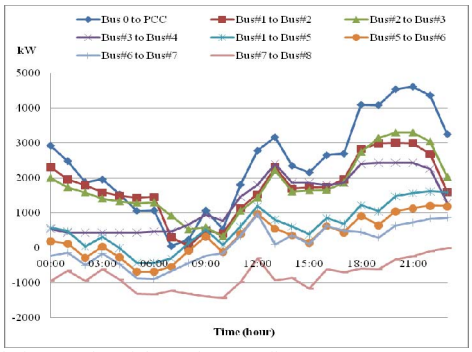

Fig. 6 Simulation results of the real power flow

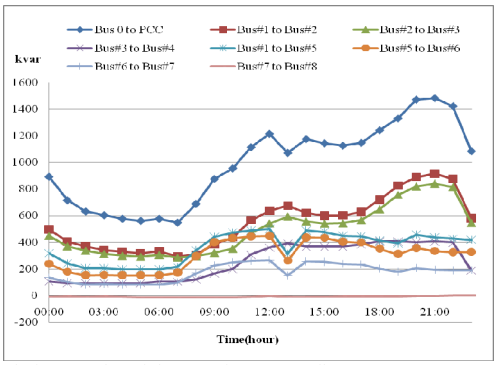

Fig. 7 Simulation results of the reactive power flow

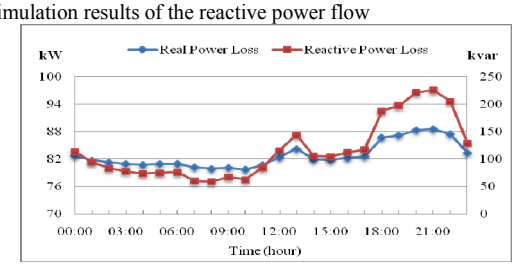

Fig. 8 Simulation results of the system losses

V. Conclusions

In this paper, a detailed power flow analysis of a high-voltage MG with various DRs and loads was performed. The 24-hour period voltage profiles, line flow profiles, and total system losses were explored via a sequential power flow program using the Newton-Raphson method. This program was developed in Matlab environment. The simulation results show that the incorporation of DRs is helpful in enhancing system operation performance and efficiency.

Acknowledgment

The authors would like to thank the National Science Council of the Republic of China, Taiwan, for financially supporting this research under Contract No. NSC 97-2221-E-270-014-MY3 and Contract No. NSC 97-2221-E-149-010-MY3.

References

[1] Website: http://unfccc.int/kyoto_protocol/items/2830.php.

[2] R. H. Lasseter, and P. Paigi, "Microgrid: A Conceptual Solution," IEEE Power Electronics Specialists conference on Volume 6, 20-25 June 2004, pp. 4285 – 4290.

[3] P. Piagi, and R. H. Lasseter, "Autonomous Control of Microgrids," Power Engineering Society General Meeting, IEEE, 2006.

[4] R. H. Lasseter, "MicroGrids," IEEE Power and Energy Magazine, Volume 5, issue4, pp.78 – 94, July-Aug. 2007.

[5] R. H. Lasseter, "CERTS MICROGRID," Electrical Engineering Department University in Wisconsin-Madison Madison, U.S., 2007.

[6] F. Katiraei, R. Iravani, N. Hatziargyriou, and A. Dimeas, "Microgrids management," Power and Energy Magazine IEEE.2008,6(3), pp. 54-65.

[7] B. Scott, "Review of load-flow calculation methods," Proceedings of the IEEE, Vol. 62, No. 7, pp. 916-929, Jul. 1974.

[8] M. S. Srinivas, "Distribution load flows: a brief review," IEEE Power Engineering Society Winter Meeting, Vol. 2, pp. 942-945, Jan. 2000.